TRACKER: a Particle Image Tracking (PIT) Technique Dedicated to Nonsmooth Motions Involved in Granular Packings

Gaël Combe and Vincent Richefeu

UJF-Grenoble 1, Grenoble-INP, CNRS UMR 5521, 3SR Lab., B.P. 53, 38041 Grenoble Cedex 09, France.

Abstract. We present a new approach to assess the 2D motion of rigid bodies in granular materials. Although it was adapted from Digital Image Correlation (DIC) technique, the heart of the presented technique relies on specific treatments related to the discrete nature of grain-displacement fields. The code called TRACKER has been developed to process the digital images and measure the in-plane displacement and rotation of each individual grain from one image to another. A remarkable feature is the use of a specific strategy that allows tracking all particles, without *losing* any of them (which is a typical problem when tracking assemblies of discrete particles over many images). This is achieved by a two-step procedure, where, in case of problematic tracking of a grain, the size of the search zone is increased in an adaptive manner, *i.e.*, taking into account the results of tracking in the neighborhood of the particle. The accuracy of the measured displacements and rotations was tested on both perfect synthetic images and digital photographs of a sheared assembly of grains. The accurate assessment of the grain kinematics opens very interesting perspectives, especially in the study of displacement fluctuations in granular media.

Keywords: Digitial Image Correlation, Sub-Pixel, Discrete Materials, Kinematic Assessment, Precision Evaluation
PACS: 42.30.Va, 42.30.Sy, 45.70.-n

INTRODUCTION

The shear apparatus named $1\gamma 2\varepsilon$ [1] and developed at the 3SR Laboratory–Grenoble is a two-dimensional parallelepiped that allows for any quasi-static straining on a Schneebeli 2D granular analogue materials, Figure 1.

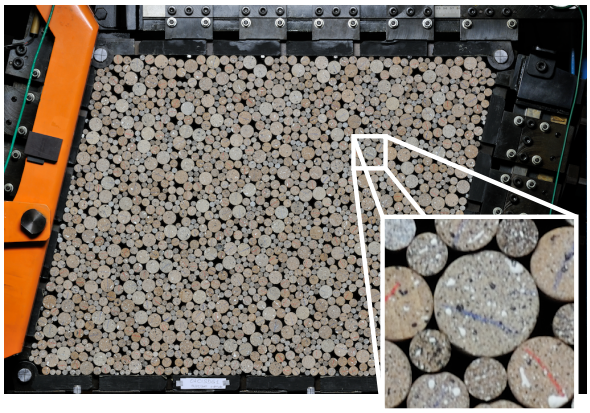

FIGURE 1. Assembly of about 2000 rods in $1\gamma 2\varepsilon$ shear device [1]. Initial size of the packing: 55×60 cm. Mean diameter of the rods: ~ 13 mm.

It has been used to study, for instance, the structure evolution of granular materials under complex loading paths [2] or the effect of shape effect [3]. One particularity of this device is that the front face of the specimen is exposed. During tests, pictures are shot and then analyzed to extract full 2D kinematics of individual grains. In the 90's, this extraction was performed by means of 12×9 cm silver photographies in which particle translations and rotations were manually measured using an stereocomparator device. The displacement (translation) accuracy was quite good (in the order of $3 \cdot 10^{-3}$ mean diameter), but the time required to treat each photograph was prohibitive (typically 1.5 hours per photo to manually click on 1000 rods). At the start of this century, analogue cameras were replaced by digital cameras. Thus, a new numerical photogrammetry technique to obtain semi-automated measurements of kinematics was used [4]. The use of digital cameras made the shots easier (no need of the photography silver film processing step), however the image analysis procedure proposed by [4] was not able to reduce the process time: between each couple of successive pictures, even if most particles *move* almost like continuum mechanics dictates, many of them have unpredictable displacements and it was necessary to manually "help" the process to find the right position and rotation of grains. Moreover, the accuracy was very coarse (in the order of the pixel, which correspond to 10^{-2} of particle's mean diameter with the 16 Mpixels digital camera used at this time).

It was therefore decided to develop a new way to assess full 2D kinematic from digital photographs of granular samples made of Schneebeli rods with the following specifications: fully automated measurement of grain kinematic (translations and rotations) able to handle more than 1000 digital photographs and above all, a displacement accuracy strongly increased compared to that obtained by [4].

THE PIT TECHNIQUE

Over the last few years, there has been substantial development in quantitative imaging analysis. One of them is the *digital image correlation* (DIC), initially suggested by [5]. It has become a powerful technique that provides reliable kinematic measurement fields, *e.g.*, displacement, acceleration, strain, strain-rate fields. This technique is a fully non-intrusive measurement tool that can be used to follow the straining of patterns of a wide range of materials such as metals, polymers, ceramics, concretes and granular materials [6]. The latter can be treated as continuous when the followed pattern includes several grains [7]. However, problems arise when the DIC is applied at the grain scale: the motion of individual grain is not regular due to geometric mutual exclusion, and it does not strictly mirror the kinematics imposed at the packing boundaries [8, 9].

We have developed an image processing software called TRACKER where the in-plane displacement vectors are obtained by a technique based on DIC. The speckles on a digital image of each grain are used to track their displacements u, v and orientation θ from their original position $\mathbf{r_0} = [r_x, r_y]$. Tracked patterns are sets of pixel position $\mathscr{S}_1 = \{x_1, y_1\}$ relative to $\mathbf{r_0}$ (in most cases, center of the grains). Gray levels held by each pixel of the pattern represent an optical signature, which is a local signal used to compute a cross-correlation (CC) coefficient. Among various definition of CCs, the *zero-mean normalized cross-correlation* (ZNCC) coefficient is used for its robustness:

$$ZNCC = \frac{\sum_{\mathscr{S}_1}[I_1(x_1,y_1)-\bar{I_1}][I_2(x_2,y_2)-\bar{I_2}]}{\sqrt{\sum_{\mathscr{S}_1}[I_1(x_1,y_1)-\bar{I_1}]^2 \sum_{\mathscr{S}_1}[I_2(x_2,y_2)-\bar{I_2}]^2}}, \tag{1}$$

where I_n is the gray level of the pixel of coordinates (x_n, y_n) of the picture n and $\bar{I_n}$ is the mean gray level computed over the corresponding pixel subsets $\mathscr{S}_n$. (x_2, y_2) are coordinates of the pixel subset on the deformed picture 2. In the case of rigid motions, the relationship between $\mathscr{S}_1 = \{x_1, y_1\}$ and $\mathscr{S}_2 = \{x_2, y_2\}$ is such that

$$x_2 = x_1 + u + (x_1 - r_x)\cos\theta - (y_1 - r_y)\sin\theta \tag{2}$$

$$y_2 = y_1 + v + (x_1 - r_x)\sin\theta + (y_1 - r_y)\cos\theta \tag{3}$$

The tracking procedure consists in finding for each grain position $\mathbf{r_0}$, the displacements u, v and the rotation θ so that the ZNCC between a pair of signals from two distinct images is maximized (in practice we minimize 1 - ZNCC). To obtain a sub-pixel resolution, the signal from second image has to be built from interpolated values of grey levels over the subset $\mathscr{S}_2$. The software implements bilinear and bicubic functions to perform the interpolation, partial derivatives being computed by centered finite differences. To find the values of $[u, v, \theta]$ that best optimize ZNCC, the *Powell*'s conjugate direction method [10] is used. This method does not need to define a function for the gradient of ZNCC, but as for other optimization techniques, a "good" starting point is required. We chose this point by testing a set of plausible positions and orientations picked from a rectangular search-zone centered on the tracked point that rotates incrementally. The best starting point has the largest ZNCC and gives an estimate of position with a pixel resolution. Sometimes, due to the granular nature of the sample, a particle can be far from its expected position. A rescue procedure is implemented to solve this problem by increasing the search-zone (including the angular degrees of freedom). A second increase of the search-zone is done if the first rescue attempt is unsuccessful. One can imagine that this procedure slows down the tracking. Fortunately, it is dramatically accelerated when prohibited zones defined by well-found neighbors are taken into consideration, Figure 2.

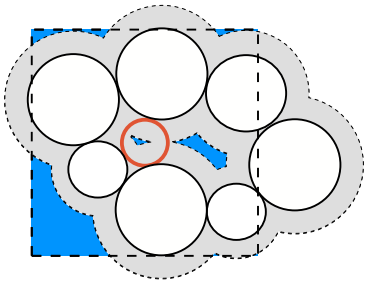

FIGURE 2. Scketch of a rescue procedure. White grains are already well correlated and the reds need "rescuing" because of its large displacement between two picture shots. The dashed box is the rectangular search-zone that was increased to find the red grain after a first unsuccessful attempt with a very small search-zone. Taking in account steric exclusions (light grey zones) due to the local geometry of the assembly of particles and the diameter of the red grain, the blue spaces are places were the center of the red grain could be. In practice, the blue zone is less the 5% of the area associated to the rectangular search-zone.

Moreover, most numerical procedures during the tracking can be applied for each grain regardless of the others. This makes the parallelization very easy to implement and the CPU time was observed to be almost linearly dependent on the numbers of CPU cores.

To avoid accumulation of digital truncation errors in the sequential processing of the photographs, we took benefits of the rigid nature of the motion, that is the fact that the pattern remains unchanged after the transformation (translation and rotation, but no distortion). Thus, the CCs was not performed between successive photographs $(n \to n+1)$. Instead, they were directly carried out between the first and the current photographs $(1 \to n)$ so that no digital truncation error occurs. This solution can be completed efficiently if the transformation $1 \to n-1$ is already known.

ACCURACY WITH IDEALIZED IMAGE

TRACKER accuracy was estimated by following $n = 400$ points spatially distributed on synthetic images from [11]. The synthetic images simulate the rigid motion of a Speckle-texture captured by an idealized camera (perfect sensors with fill-factor equals to 1), Figure 3.

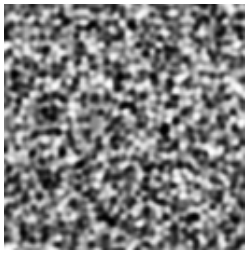

FIGURE 3. Synthetic speckle-pattern image [11]– courtesy, L. Robert.

Two image series with two kinds of transformation were independently generated: pure translation and pure rotation. We tested the dependence of the sub-pixel translation and rotation accuracy with respect to the degree of the polynomial function (bilinear or bicubic) used to interpolate the image and the size (pixels) of the squared pattern interpolated.

Translations – An imposed displacement $u^\bullet$ was varied from 0 to 1 pixel with a step of 0.02 pixel. We compared $u^\bullet$ with the corresponding displacement u_i of each of the 400 points i followed to determine their displacement error: $\Delta u_i = u^\bullet - u_i$. The arithmetic mean of Δu_i defined the systematic error (or bias), $\langle \Delta u \rangle = \frac{1}{n}\sum_{i=1}^{n} \Delta u_i$. In addition, the standard deviation (random error) σ_u was computed.

As for other accuracy studies [12, 13], displacements were evaluated at all positions of a regular square grid in the initial image, with a pitch such that correlation windows at adjacent positions do not overlap, ensuring the statistical independence of the corresponding errors.

Figure 4 shows the bias and the random error obtained for imposed translations $u^\bullet$ in the horizontal direction. Although the bias is almost independent of the pattern size, the random error is decreased with the size of the pattern, whatever the degree of the interpolation function. These results are consistent with those of [12, 13]. For a given pattern size, random errors are smaller for bicubic than for bilinear interpolations. For example, the worst accuracy in translation for the largest pattern (33×33) is 0.0005 ± 0.0013 pixel with bilinear interpolation and 0.0126 ± 0.0012 pixel with bicubic interpolation. Thus, the bilinear interpolation seems the better choice (for large patterns) in term of accuracy in the displacement, with the use of synthetic images.

Rotations – The imposed rotations were varied from

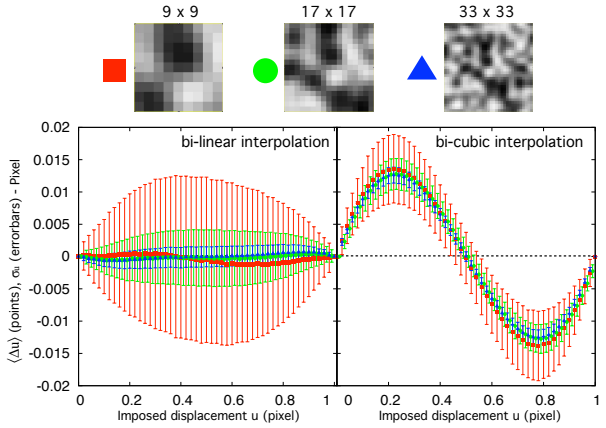

FIGURE 4. Horizontal translation accuracy as a function of the imposed displacement $u^\bullet$. Bias error (symbols) and random error (vertical error bars) with different pattern sizes (on the top) and interpolating functions (bilinear on the left, bicubic on the right).

0 to 180 degrees by increment of 5 degrees. The bias error $\langle \Delta\theta \rangle$ and the random error σ_θ for rotations was determined in the similar manner as for the translations. Provided that the pattern contains a sufficient number of pixels (33×33), the bias $\langle \Delta\theta \rangle$ is not very sensitive to the degree of the interpolation function used, Fig. 5.

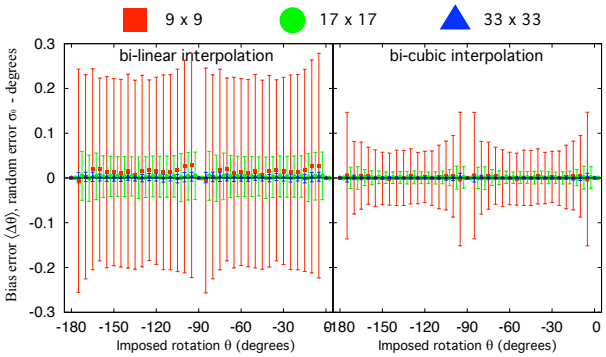

FIGURE 5. Accuracy in rotation as a function of the imposed rotation. Bias error (symbols) and random error (vertical error bars) with different pattern sizes (on the top) and interpolating functions (bilinear on the left, bicubic on the right).

For the random errors σ_θ, the same observations as for the translation accuracy analysis can be made: the smallest value of σ_θ is observed for bicubic interpolation. Moreover, σ_θ is three times smaller when the number of pixels in the pattern is approximatively four times bigger. This is understandable when one considers that a rotation implies pixels translation so that the rotation angle is of the order of $\tan^{-1}(\ell/d)$, where d is the distance of each pixel to the center of rotation and ℓ is its displacement length. For a given error on ℓ, it is worth noting that bigger values of d (corresponding to $\sqrt{2}/2$ the squared pat-

tern size) leads to smaller errors on the rotations. For the specific rotations of 90 and 180 degrees, $\langle \Delta\theta \rangle$ and σ_θ were so small (lower than 10^{-8} degrees) that they were out of reach. Finally, TRACKER is able to track rotations with a maximum error of 0.0024 ± 0.0106 degrees using a pattern size of 33×33 pixels with bilinear function of interpolation, and 0.0021 ± 0.0085 degrees with bicubic function.

ACCURACY WITH REAL IMAGES

For real images of moving bodies coming from a digital camera, the estimate of the error for displacements and rotations is rather complex because it implies a perfect mastery of the whole measurement chain. However, error measurements can be highlighted by an indirect approach: in a granular material, two segments of known length $S_0 = 60$ pixels and initially perpendicular are placed on a number of particles (inset of the figure 6). Assuming perfectly rigid particle, these segments must remain perpendicular in pairs and of constant length in spite of the large displacements and rotations of the particles. The accuracy study is here performed over 24.5 Mpixels pictures of an assembly of about 2000 rods submitted to a quasi-static shear ing (Fig. 1), $\dot{\gamma} = 8.2 \times 10^{-5}$ s^{-1}. Along the shear test, pictures are shot every 5 seconds. The correction of optical distortion which requires a specific procedure (not explained here due to space limitations) was performed for in the study. If not, measured accuracy would be at least two times worse. Figures 6(a) and 6(b) show the bias and random error of the measured variations of length ΔS and angle $\Delta\alpha$, respectively, throughout the shear test – obtained by comparing each image to the initial one. It is shown that $\Delta S = 0.01 \pm 0.05$ pixel (corresponding to $1.1 \times 10^{-3} \pm 5.5 \times 10^{-3}$ mm for our configuration) and $\Delta\alpha = 0.01 \pm 0.06$ degrees.

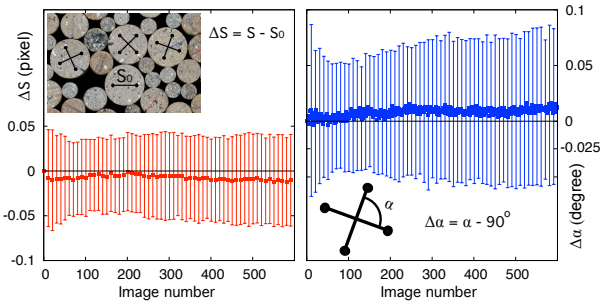

FIGURE 6. Accuracy for particle tracking with real photographs of a $1\gamma 2\varepsilon$ shear test. (a) bias (symbols) and random error (vertical error bars) of changes of length ΔS measured on 434 segments; (b) bias (symbols) and random error (vertical error bars) of changes of angle measured on 217 pairs of initially perpendicular segments.

CONCLUSIONS

A new parallelized code called TRACKER dedicated to the tracking of nonsmooth trajectory of particles was presented. The software uses the digital image correlation technique coupled with geometrical rules to dramatically increase the efficiency of the cross-correlations. These tremendous improvements allow for an accurate and fast assessment of the grain kinematics without "losing" any of them. The proposed strategy was successfully used – at the time of writing this short paper – to exhibit very interesting features of particle fluctuations in sheared dense granular systems [8, 9].

ACKNOWLEDGMENTS

The authors thanks L. Robert, member of the Workgroup "Metrology" of the French CNRS research network 2519 for his help on the synthetic speckled images. A special thanks to Dr. S. A. Hall for interesting and fruitful discussions. Thanks to E. Andò for his careful reading to improve this paper.

REFERENCES

1. H. Joer, J. Lanier, J. Desrues and E. Flavigny, *Geotechnical Testing Journal*, **15**(2):129–137 (1992).
2. F. Calvetti, G. Combe and J. Lanier, *Mechanics of Cohesive Frictional Materials*, **2**(2):121–163 (1997).
3. E.-M. Charalampidou, G. Combe, G. Viggiani and J. Lanier, *Powders and Grains 2009*:821–824 (2009).
4. L. Sibille and F. Froiio, *Granular matter*, **9**:183–193 (2007).
5. T. C. Chu, W. F. Ranson, M. A. Sutton and W. H. Peters, *Experimental Mechanics* **25**(3):232–244 (1985).
6. E. Andò, S. A. Hall, G. Viggiani, J. Desrues and P. Bésuelle, *Géotechnique Letters*, **2**:107–112 (2012).
7. S.A. Hall, D. Muir Wood, E. Ibraim and G. Viggiani, *Granular Matter*, **12**(1):1–14 (2010).
8. V. Richefeu, G. Combe and G. Viggiani, *Géotechnique Letters*, **2** (july–september):113–118 (2012).
9. G. Combe, V. Richefeu, G. Viggiani, S.A. Hall, A. Tengattini and A.P.F. Atman, *Powders and Grains 2013*:xxx–xxx (2013).
10. W. H. Press, S. A. Teukolsky, W. T. Vetterling and B. P. Flannery, *Numerical Recipes 3rd Edition: The Art of Scientific Computing*, Cambridge University Press (2007).
11. J-J Orteu, D. Garcia, L. Robert and F. Bugarin, *Proc. SPIE 6341, Speckle06: Speckles, From Grains to Flowers, 63410H* (September 15, 2006); doi:10.1117/12.695280 (2006).
12. N. Bornert, F. Brémand, P. Doumalin, J.-C. Dupré, M. Fazzini, M. Grédiac, F. Hild, S. Mistou, J. Molimard, J.-J. Orteu, L. Robert, Y. Surrel, P. Vacher and B. Wattrisse, *Experimental Mechanics*, **49**(3):353–370 (2009).
13. J.C. Dupré, M. Bornert, L. Robert and B. Wattrisse, *EPJ Web of Conferences*, **6**:31006 (2010).